Non-steady state diffusion and advection model of transient concentration-depth profiles from the Barbados Accretionary Complex

Numerical model
Interstitial water
Diffusion
Advection
Diagenesis

Modèle numérique
Eau interstitielle
Diffusion
Advection
Diagenèse

Gérard BLANC [a], Claude DOUSSAN [b], Catherine THOMAS [c] and Jacques BOULEGUE [d]

[a] Centre de Géochimie de la Surface (UPR 6251), Institut de Géologie de Strasbourg, Université Louis Pasteur, 1, Rue Blessig, 67084 Strasbourg Cedex, France.

[b] Centre d'Informatique Géologique, École Nationale Supérieure des Mines, 35, rue Saint-Honoré, 77305 Fontainebleau, France.

[c] Groupe de Recherches en Géodésie Spatiale, UMR 39, Centre National d'Études Spatiales, 18, avenue Édouard Belin, 31055 Toulouse Cedex, France.

[d] Laboratoire de Géochimie et Métallogénie, Université Pierre et Marie Curie, URA CNRS 196, 4, place Jussieu, 75252 Paris, France.

Received 3/12/92, in revised form 25/05/93, accepted 3/07/93.

ABSTRACT

We present a non-steady-state diffusion and advection model that describes the distribution of methane, manganese and silica concentrations *versus* depth at sites 671, 676, and 672 of ODP Leg 110 through an oceanic sedimentary pile undergoing horizontal shortening by means of thrust-faults and folds. The model suggests that the distribution of these chemical components above and below fluid flow conduits is controlled by molecular diffusion. Upward fluid advection from the pathways to the surrounding sediments appears to be without significance for this environment (about 1.10^{-11} m.s^{-1}, *i.e.* ≈ 0.3 mm.yr^{-1}). Estimates of the time necessary to produce the diffusion profiles indicate that average ages of the chemical anomalies increase from Site 672 to Site 671, *i.e.* from the oceanic domain towards the internal part of the accretionary prism. Using a two-dimensional framework for the model, fluid-flow velocities along the décollement and protodécollement zones are estimated about 7.10^{-9} m.s^{-1} (*i.e.* ≈ 0.20 m.yr^{-1}) and 1.10^{-7} m.s^{-1} (i.e. ≈ 3 m.yr^{-1}), respectively. Comparisons between ion-activity products of rhodochrosite and amorphous silica, and their equilibrium constants suggest the dissolution of biogenic silica and precipitation of rhodochrosite within the décollement zone, which is the major fluid conduit of the Barbados Accretionary Complex.

Oceanologica Acta, 1993. **16**, 4, 363-372.

RÉSUMÉ

Modélisation en régime transitoire des processus de diffusion et d'advection dans les eaux interstitielles du prisme d'accrétion de la Barbade: traitement des profils concentration-profondeur

Dans cet article, nous présentons un modèle de diffusion-advection en régime transitoire rendant compte de la distribution en fonction de la profondeur des

concentrations en méthane, manganèse et silice dissoutes dans les eaux interstitielles prélevées dans les sites 671, 676 et 672 du Leg 110 ODP. Cette modélisation suggère que la distribution de ces espèces chimiques de part et d'autre des conduits structuraux et lithologiques permettant la circulation de fluide, est essentiellement contrôlée par le processus physique de diffusion moléculaire. La vitesse d'advection ascendante depuis ces conduits vers les sédiments environnants est non significative dans ce contexte, de l'ordre de 1.10^{-11} m.s^{-1} ($\approx$ 0.3 mm.an^{-1}). Les estimations du temps nécessaire pour que les profils théoriques obtenus rendent compte au mieux de la distribution des données analytiques indiquent que les âges des anomalies positives observées sont de plus en plus vieux depuis le site 672 vers le site 671, c'est-à-dire du domaine océanique vers l'intérieur du prisme d'accrétion. En considérant une circulation de fluide dans les zones de décollement au niveau de la coupe géologique du leg 110 ODP, les vitesses de circulations estimées par un simple calcul sont de l'ordre de 7.10^{-9} m.s^{-1} ($\approx$ 0.20 m.an^{-1}) dans le décollement entre les sites 671 et 676 et 1.10^{-7} m.s^{-1} ($\approx$ 3 m.an^{-1}) dans le protodécollement entre les sites 676 et 672. La comparaison entre les produits d'activité ionique de la rhodochrosite et de la silice amorphe et leurs constantes d'équilibre thermodynamique suggèrent qu'au niveau des zones de décollement, la silice biogénique est dissoute et la rhodochrosite précipite.

Oceanologica Acta, 1993. **16**, 4, 363-372.

INTRODUCTION

Accretionary prisms which develop from material scraped from the subducting ocean lithosphere have been intensively investigated. Relevant results were obtained during Leg 110 of the Ocean Drilling Project (ODP) along a northern transect of the Barbados Accretionary Complex (B.A.C.; Fig. 1). The results defined the relationship between structural and hydrological processes (ODP Leg 110 scientific Party, 1987; Moore *et al.*, 1988). Geochemical anomalies strongly suggested that fluid circulation occurs along pathways controled by major tectonic structures of the accretionary wedge. These pathways are the décollement and its propagation toward the oceanic domain, and the major thrust-faults associated with detachment surfaces (Blanc *et al.*, 1988; 1991; Gieskes *et al.*, 1989; 1990 *a* and *b*). Methane, chloride and manganese were the chemical tracers used for assessing the fluid circulation (Fig. 1). Positive silica anomalies correlate well with manganese (Fig. 2), and can also be related to fluid circulation. Fluid circulation at the toe of the Barbados accretionary prism is partly related to geothermal anomalies discovered during Leg 110 (Fisher et Hounslow, 1990 *a* and *b*). The clearcut anomalies in the thermal gradients strongly support the concept that the chemical anomalies are of recent origin. The thermal gradients induce a non-steady state distribution of temperature as well as the chemical elements (Fisher et Hounslow, 1990 *a* ; Blanc *et al.*, 1991).

This paper attempts to explain the distributions of methane, manganese and silica concentrations *versus* depth with respect to fluid flow along defined structural and lithological pathways. We propose a non-steady state mathematical model to evaluate the consequences of diffusion and advection processes on the concentration-depth profiles of dis-

Figure 1

Down: cross section through the zone of initial accretion showing the location of sites 671, 676, and 672 (after Moore et al., *1988). N = Neogene; E = mid-late Eocene; O = Oligocene; S-E = Senonian-early Eocene; C = Oceanic crust; EPDOD = East Propagating Décollement toward the oceanic domain (protodécollement). Up: methane (CH4) and sulfate (SO_4^{--}) concentration-depth profiles; sites 671, 676, 672, 673 and 674.*

Bas : coupe synthétique au travers de la zone d'étude du Leg 110, montrant la localisation des sites 671, 676 et 672 (d'après Moore *et al.*, 1988). N = Néogène ; E = Eocéne moyen-supérieur ; O = Oligocène ; S-E = Sénonien-Eocène inférieur ; C = croûte océanique ; EPDOD = propagation du décollement vers l'Est dans le domaine océanique (protodécollement). Haut : profils de concentrations dissoutes en méthane et sulfate en fonction de la profondeur; sites 673, 674, 671, 676 et 672.

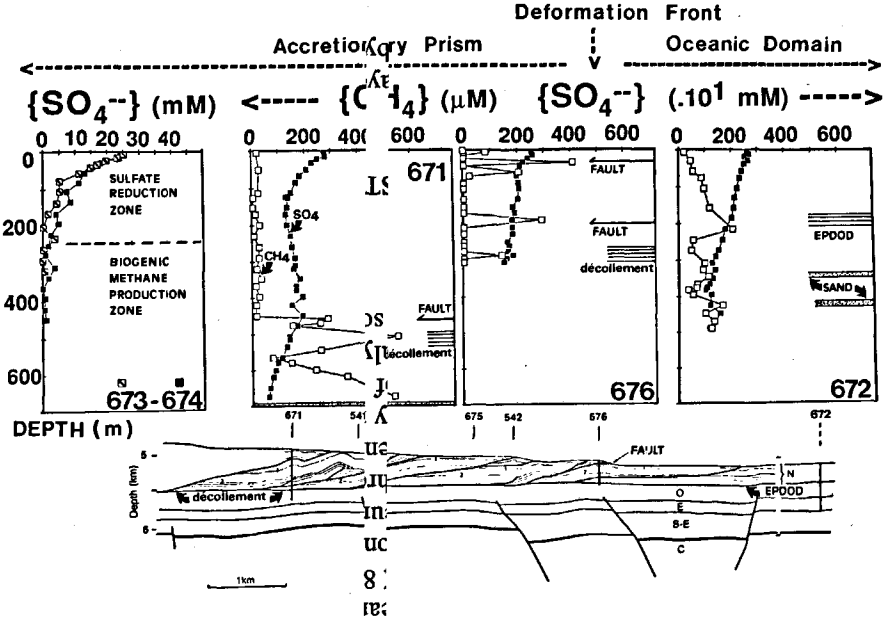

Figure 2

Concentration-depth profiles of the dissolved silica and manganese; sites 671, 676 and 672.

Profils des concentrations en silice et manganèse dissoutes dans les échantillons d'eau interstitielle en fonction de la profondeur, sites 671, 676 et 672.

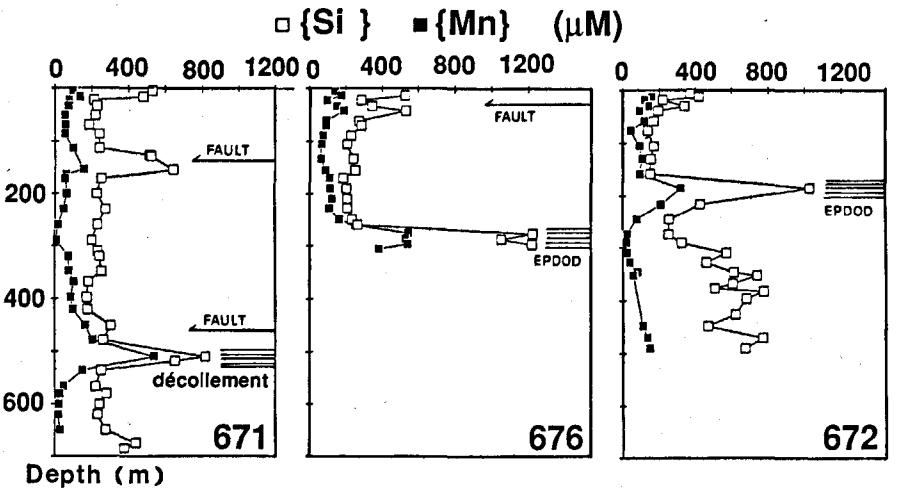

solved methane, manganese, and silica. The theoretical concentration-depth profiles are then compared to the analytical profiles, and the age of onset of the observed chemical anomalies can be deduced. Fluid flow velocities will be examined on the basis of the ages given by the model for the chemical anomalies. We will also examine the diagenetic processes induced by fluid flow, processes that eventually affect the concentrations of methane, manganese and silica dissolved in the interstitial waters.

METHODS

Determination of the chemical components used in this paper were detailed in previous papers (Blanc *et al.*, 1988; 1991; Gieskes *et al.*, 1989; 1990 *a* and *b*). The mineralogical and chemical analyses of the 110, 676A, 31X-3,145-150 cm squeezecake sample collected from the décollement zone were respectively performed by X-ray diffraction using Cu-Kα radiation, and by means of a Spectrometer Electron Microscope "SEM JSM 840". The X-ray diffraction diagram obtained on the fraction > 63 μm of this squeezecake sample revealed the occurrence of three major phases: amorphous silica, rhodochrosite and traces of albite. Quantitative analyses of elemental abundances of rhodoch,rosite particles were done by means of EDS Tracor TN 5 500 using an acceleration of 15 KV, a beam current of 10 nÅ, and a 1 μm-wide analysis area. Electron microprobe results were normalized so that the sum of Ca + Mg + Mn + Fe = 1.

GEOCHEMICAL AND STRUCTURAL CONSTRAINTS FOR THE MODEL

Figures 1 and 2 show that the more permeable layers of the front of the northern B.A.C. are characterized by positive methane, manganese and silica anomalies.

The origin of the dissolved methane in the interstitial water of sediments cored during Leg 110 improves the hypothesis of advection of fluids along the décollement and more permeable layers of northern B.A.C. Methane can be produced in nature by both microbial and thermal degradation of organic matter. At sites 671, 676 and 672, the high methane contents determined in interstitial water containing dissolved sulfate suggest that the methane sampled is not biogenically derived. On the other hand, the lack of methane observed at sites 673 and 674 below the sulfate reduction zone also indicates that no biological methane production occurs in these sites (Gieskes *et al.*, 1989). Both the very low C1/(C2 + C3) ratios (Blanc *et al.*, 1991) and the characteristic isotopic composition of methane carbon (Vrolijk *et al.*, 1990) strongly suggest a thermogenic methane production. At the depths of occurrence of methane at sites 671, 676 and 672, temperatures are not high enough for thermogenic methane to form *in situ*. Hence, we postulate that the thermogenic methane has its origin at much greater depths than that reached at site 671 and, consequently, this indicates a deep source for the fluid sampled in the décollement and associated faults and, also, in the underlying permeable sand layers.

The nature and the causes of the anomalies of Mn and Si can be discussed to explain why the décollement and the eastward propagating décollement are well characterized by positive manganese and silica anomalies (Fig. 2). Syntectonic carbonate veins were discovered at four sites [sites 673, 674, 675 and 676 (Schoonmaker-Tribble, 1990; Vrolijk and Sheppard, 1991)]. Veins from sites 675 and 676 occur in the décollement zone at the deformation front. The mineralogical and chemical analyses of a sample collected from the décollement zone in the hole 676A have been done in this study. Description of the morphology and qualitative analyses by SEM indicate that this sample is essentially composed of radiolarian fragments and radially fibrous spheroid rhodochrosite. The average values of the relative cation abundances based on multiple analyses of individual rhodochrosite grains is given in the following percentages: Mn = 92.78 ± 3.32, Mg = 4.57 ± 0.31, Ca = 2.65 ± 0.35, Fe = 0.00. This result indicates low contents of magnesium and calcium substitute for manganese, but with no detectable iron. The chemical composition of the rhodochrosite is relatively constant from core to border of the studied grains. This suggests that the chemical composition of the flowing fluid probably did not significantly change during the precipitation of the rhodochrosite particles. A

similar rhodochrosite elementary composition was also found in the 110-676-33X-1, 22-29 cm sample (Vrolijk and Sheppard, 1991). The presence of crystals of rhodochrosite in the early Miocene radiolarian-rich claystones of the protodécollement zone at the most seaward edge of the accretionnary wedge (site 676) is associated with positive silica and manganese anomalies in interstitial water. The characteristics of manganese and silica concentration-depth profiles might be due to variations in dissolved manganese and silicic acid contents, and equilibrium with rhodochrosite and amorphous silica. A test of this possibility can be done by assessing whether conditions of deposition of rhodochrosite and amorphous silca are reached in the interstitial fluid. This is made by comparing the ion activity products (Q) of rhodochrosite and amorphous silica with the related equilibrium constants (K). In our calculations, we have corrected the latter for rhodochrosite and amorphous silica for *in situ* temperature and pressure. The computation was done for 671, 676 and 672 interstitial water samples on the basis of the shipboard and shore-based laboratory analyses (Gieskes *et al.*, 1990; Blanc *et al.*, 1991). The activity coefficients and the ion association distribution were determined using the thermodynamic code Equil-T (Fritz, 1981). The results are given in Figures 3 and 4 for sites 671, 676 and 672. These diagrams show that all the interstitial water samples are under-saturated with respect to amorphous silica, as are several samples with respect to rhodochrosite. Only the water samples collected at the décollement zone are over-saturated relative to rhodochrosite formation. Thermodynamic tests considering pyrolusite and manganosite as manganese-oxide minerals indicate that all interstitial water samples are greatly under saturated with respect to these minerals. These thermodynamic results suggest that the most positive anomalies of the dissolved silica and manganese are essentially controlled by the dissolution of amorphous silica and the precipitation of rhodochrosite, respectively. On the other hand, Vrolijk and Sheppard (1991) described small spheroids of radially fibrous carbonate around an MnO_x core. This suggests that MnO_x reduction may be the major process leading to an increase of the Mn^{2+} concentrations in the interstitial water. The dissolution of biogenic silica probably acts as an additional source of dissolved manganese. Where sursaturation with respect to rhodochrosite is reached, precipitation occurs. These results imply that the flowing fluid has reducing properties.

Thus, fluid circulation is directly or indirectly responsible for the observed positive methane, manganese, and silica anomalies. In this case, the distribution of these chemical components above and below the fluid conduits, might be controlled by physical processes such as molecular diffusion and eventually upward fluid advection from the pathways to the surrounding sediments. A non-steady state model is proposed to obtain transient theoretical profiles of the rate of diffusion, and eventually, of the upward secondary advection processes in the sediment prism. The first constraint for this model is the location of the fluid

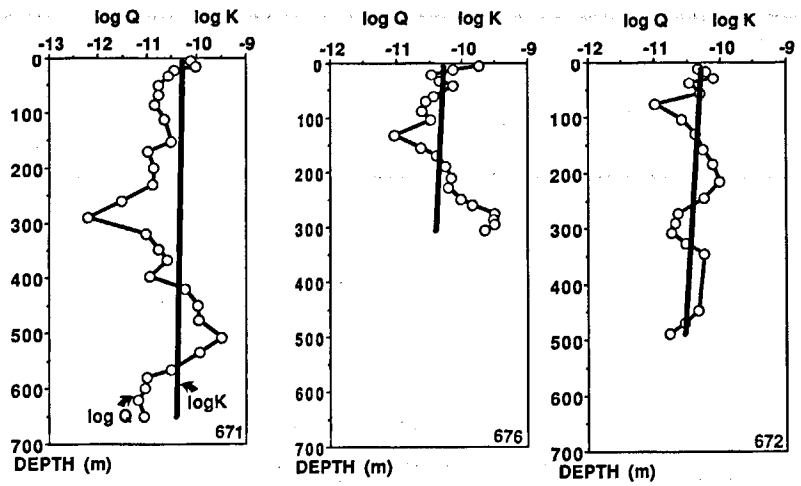

Figure 3

Diagrams showing a comparison between the log profiles of the ion activity products (log Q) and those of the thermodynamic equilibrium constant (log K) of rhodochrosite; sites 671, 676 and 672.

Diagrammes montrant la comparaison entre les profils en log des produits d'activité ionique (log Q) et ceux de la constante thermodynamique d'équilibre (log K) de la rhodochrosite, sites 671, 676 et 672.

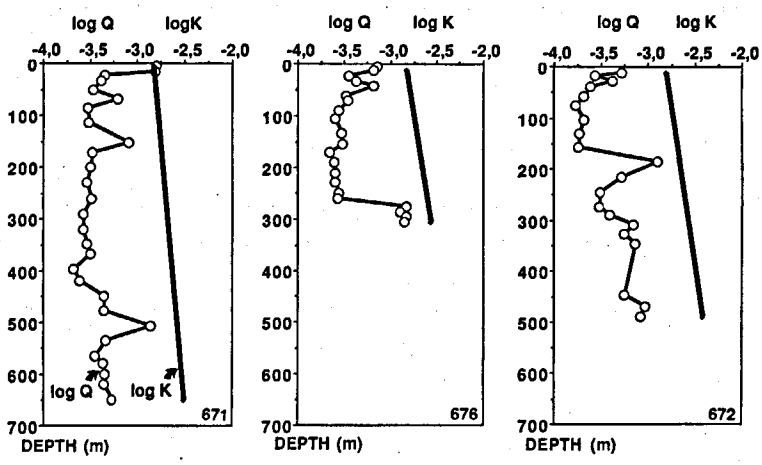

Figure 4

Diagrams showing a comparison between the log profiles of the ion activity products (log Q) and those of the thermodynamic equilibrium constant (log K) of amorphous silica; sites 671, 676 and 672.

Diagrammes montrant la comparaison entre les profils en log des produits d'activité ionique (log Q) et ceux de la constante thermodynamique d'équilibre (log K) de la silice amorphe, sites 671, 676 et 672.

conduits between which physical dispersion occurs. In the model, these fluid conduits mark the boundaries of each considered vertical slab of the sedimentary sequence. These boundaries can be related to various tectonic structures and to three characteristic lithological layers. The tectonic structures correspond to the well defined significant thrust faults and the small-scale tectonic structures such as scaly fabrics, discrete faults or veins (Berhmann *et al.*, 1988; Brown *et al.*, 1990; Brown and Berhmann, 1990). The three lithological layers are: 1) the Miocene radiolarian-rich mudstone characterizing the décollement zone at site 671, and its propagation in the oceanic domain at sites 676 and 672, and also the early Eocene radiolarian-rich mudstone in the deepest part of site 672; 2) the sand layers in the deepest part of site 672; and 3) the ash-bearing layers in the shallowest part of this site. The locations of these fluid conduits bounding the vertical slab are shown in Figures 8, 9 and 10. Sometimes, fluid conduits are not located at a point corresponding to a interstitial water sample. In this case, the corresponding concentrations have been evaluated in response to the theoritical diffusion profiles obtained both above and below the structural and lithological pathways.

THE DIFFUSION-ADVECTION MODEL.

For a fluid circulating in a porous medium, the dispersal equation is :

$$\mathrm{div}\,(w.D_b.\overrightarrow{\mathrm{grad}}c - c.\vec{u}) = w_c.\,\partial c/\partial t + (w-w_c)\,\partial c'/\partial t \qquad (1)$$

in which c is the mass concentration, in moles/m^3, of a chemical component dissolved in the pore water, moving by vertical advection, c' is the mass concentration of a chemical component dissolved in the pore water which is not involved in vertical advection, t is the time (s), D_b is the molecular diffusion coefficient in the bulk sediment (m^2/s), w_c is the kinematic porosity (%), w is the porosity, as the volume fraction occupied by flowing water (%), and u is Darcy's velocity (m/s)

We first assumed that the concentration of the chemical components is identical in both advecting and non-advecting pore water (c = c'). The dispersal equation can be written :

$$\mathrm{div}\,(w.D_b.\overrightarrow{\mathrm{grad}}c - c.\vec{u}) = w.\,\partial c/\partial t \qquad (2)$$

We then postulated that the porosity and the molecular diffusion coefficient are constant for a vertical slab of the sedimentary sequence.

Thus, equation (2) becomes :

$$D_b.\mathrm{div}\,(\overrightarrow{\mathrm{grad}}c - (c/w).\vec{u}) = \partial c/\partial t \qquad (3)$$

and for a one-dimensional axis (x) :

$$\underset{\text{diffusive term}}{D_b.\,\partial^2 C/\partial x^2} - \underset{\text{advective term}}{\mu.\,\partial c/\partial x} = \partial c/\partial t \qquad (4)$$

where x is the thickness (m) of a considered slab of the sedimentary sequence. $\mu = u/w$ which corresponds to the velocity of the interstitial water in the pore medium.

Resolution

The specific problem considered is that of a semi-infinite medium having a plane source at x = 0. Initially a saturated flow of fluid of concentration, C = 0, takes place in the medium. At t = 0, the concentration of the plane source is instantaneously changed into $C = C_b$. Thus, the appropriate boundary conditions are :

$C(0, t) = C_b;\ t \geq 0$
$C(x, 0) = 0;\ x \geq 0$
$C(\infty, t) = 0;\ t \geq 0$

The problem is then to characterize the concentration as a function of (x) and (t). To solve this problem, we can write the equation (4) in terms of the error function (Ogata and Banks, 1961):

$$C(x,t) = C_b^{0,5}\,.\,\mathrm{erfc}\{(x - \mu.t)/(2.(D_b.t)^{0,5})\} + \exp.\{(\mu.x)/D_b)\}\,.\,\mathrm{erfc}\,\{(x + \mu.t)/(2.(D_b.t)^{0,5}\} \qquad (5)$$

In studying the dispersional processes in a finite medium, the concentrations are imposed at the two extremities of a sedimentary slab, and the boundary conditions become :

$C(x, 0) = C_b$ ou $C_1;\ x \geq 0$
$C(0, t) = C_b;\ t \geq 0$
$C(x, t) = C_1;\ t \geq 0$

In using the "image" method (De Marsily, 1981), the equation (5) becomes :

$$C(x, t) = \sum_{n=1}^{\infty} \{(C_b - C_1)\,f(x + 2.n.D_b, t) - (C_b - C_1)\,f(-x + 2.n.D_b, t)\} + (C_b - C_1)\,f(x, t) + C_1 \qquad (6)$$

with $f(x, t) = (1/Cb).\,C(x, t)$

Numerical applications

To obtain the transient theoretical profile, we had further to define the studied system.

Thus, we assumed:

1) a homogeneous medium;

2) one-dimensional space along a vertical sedimentary sequence (*i.e.* we only computed the evolution of the diffusion and/or advection profile with time for a single vertical slab;

3) the initial concentrations (C_b) of the solutes were considered to be constant over a vertical slab of the sedimentary sequence, as shown in Figure 5 *i*, C_b being constant at t_0 between the depths P_1 and P_2, which define the vertical space boundaries of the system ;

4) at t_0, an anomalous concentration (C_1) appears at a defined level of the sedimentary column (P_2), for instance, lateral supply of a methane-rich fluid. This anomalous concentration remains constant until the period of the observations.

As shown in Figure 5 *i*, we have:

at t_0; C_b for $P_1 \leq x \leq P_2$; and
C_1 at $x = P_2$.

In using the following parameters, a molecular diffusion coefficient in the bulk sediment (D_b) for each chemical component considered, and a vertical advection velocity

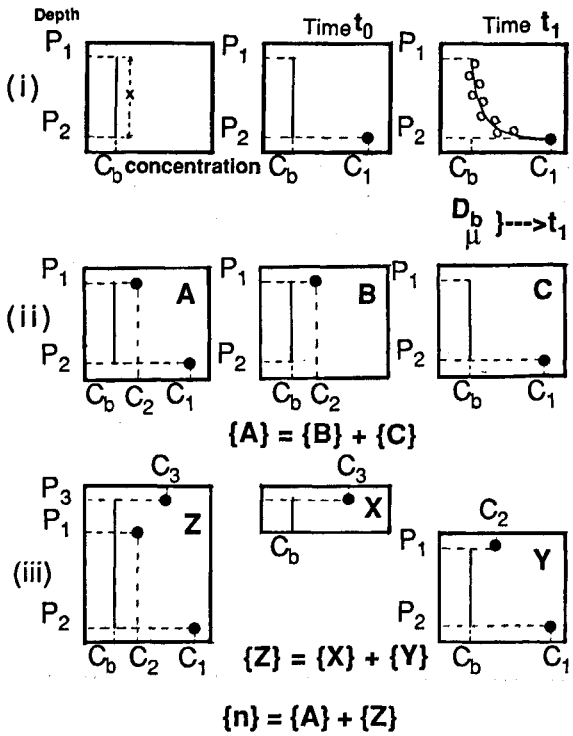

Figure 5

Diagrams showing the application model with 1, 2, 3, ... n pertubations appearing in the medium. C_b: initial concentration of the solutes in the medium, C_1, C_2, C_3, ... C_n : anomalous concentrations of the solutes appearing in the medium, at depth P_1, P_2, P_3, ... P_n. a) at t_0, an anomalous concentration (C_1) appears at depth (P_2). With D_b and μ parameters, we attempt to define a time (t_1) necessary to obtain a fitting of theoritical on analitycal profiles; b) modelling condition considering two anomalous concentrations (C_1 and C_2) appearing in the medium (see text). c) modelling condition considering three anomalous concentrations (C_1, C_2 and C_3) appearing in the medium (see text).

Diagrammes montrant l'application du modèle en considérant 1, 2, 3, ... n perturbations apparaissant dans le milieu. C_b: concentrations initiales des solutés dans le milieu, C_1 , C_2, C_3, ...C_n concentrations anormales apparaissant dans le milieu. a) à t_0, une concentration anormale apparaît à un niveau défini (P_2) de la colonne sédimentaire, causée par exemple par un apport latéral de fluide riche en méthane. Avec les paramétres D_b et μ, nous pouvons essayer de définir le temps nécessaire (t_1) pour obtenir un profil théorique rendant compte de la distribution des données analytiques en fonction de la profondeur ; b) si à t_0, deux concentrations anormales apparaissent à (P_1) et (P_2), la résolution du système correspond à la superposition de deux problèmes linéaires, la solution (A) résulte de l'addition des solutions (B) et (C).; c) si à t_0, une troisième concentration anormale apparaît à (P_3), la résolution du système peut être obtenue en découpant la colonne sédimentaire en tranches indépendantes. Pour chaque tranche, la résolution est indépendante, ainsi les paramètres D_b, μ, t peuvent être modifier.

(μ) of the interstitial water, we tried to define the time required to obtain theoretical profiles comparable to the analytically-determined concentration-depth profiles.

If at t_0, a second anomalous concentration (C_2) appears at x = P_1, we can consider the system as a superposition of two linear problems. In Figure 5 *ii*, note that solution (A) results from the addition of the solutions (B) and (C).

If at t_0, a third anomalous concentration is involved at x = P_3, the solution of the problem can be obtained in using a separation in the independent slabs of the sedimentary column. For each slab, the solution is independent, thus the parameters D_b, μ, t can be changed (Fig. 5 *iii*).

For each solute, C_b values are fixed with respect to the average of the concentration values determined far from the zone of the lateral flow.

C_1, C_2, ..., C_n correspond to the anomalous concentrations of the dissolved components at the fluid conduits, kept constant at a site-determined level.

Diffusion and porosity

Values for the molecular diffusion coefficient (D_0) of methane, manganese and silica are known in sea water as a function of temperature (Li and Gregory, 1974; Lerman, 1979). The molecular diffusion coefficients of the dissolved species in the bulk sediment (D_b) can be related to the porosities and tortuosities of sediments by means of a quantity known as the formation factor (F) (Archie, 1942; Klinkenberg, 1951; Bear, 1972; Manheim and Waterman, 1974).

$$F = R_{sed}/R_{i.w.} \quad (7)$$

where R_{sed} is the specific resistivity of the wet sediment and $R_{i.w.}$ that of the interstitial water (ohms), and :

$$D_b = D_0/\theta.F = D_0/\Phi^2 \quad (8)$$

(Manheim and Waterman, 1974)

$$\rightarrow \Phi^2 = \theta.F$$

where θ is the porosity, and Φ the tortuosity.

Porosity values are known every < 5 m along the sedimentary sequences of sites 671, 676 and 672. However, formation factor data are less abundant (Mascle *et al.*, 1988). The formation factor can also be determined as a function of the porosity, with following equation:

$$F = \theta^{-n} \quad (9)$$

(Manheim, 1970).

where n is the Archie coefficient which is related to the mineralogical composition of the sediment. The D_b value can then be determined as:

$$D_b = D_0 . \theta^{n-1} \quad (10)$$

Values for the molecular diffusion coefficient (D_b) at each depth can be determined in using following parameters: the

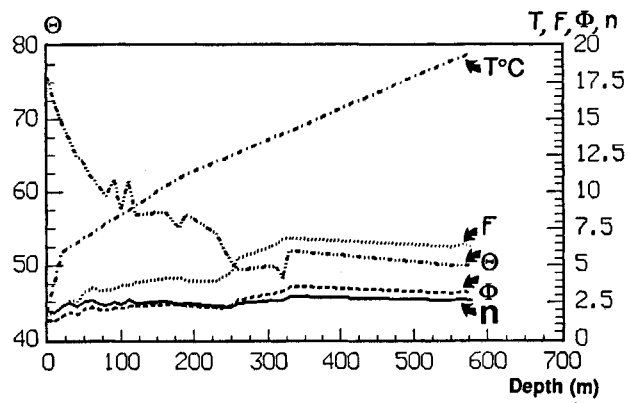

Figure 6

Diagram showing the variation of the parameters: Archie coefficient (n), tortuosity (Φ), porosity (θ), formation factor (F) and temperature (T) versus depth; Site 671.

Diagramme montrant la variation en fonction de la profondeur des paramètres: coefficient d'Archie (n), tortuosité (Φ), porosité (θ), facteur de formation (F) et température (T); Site 671

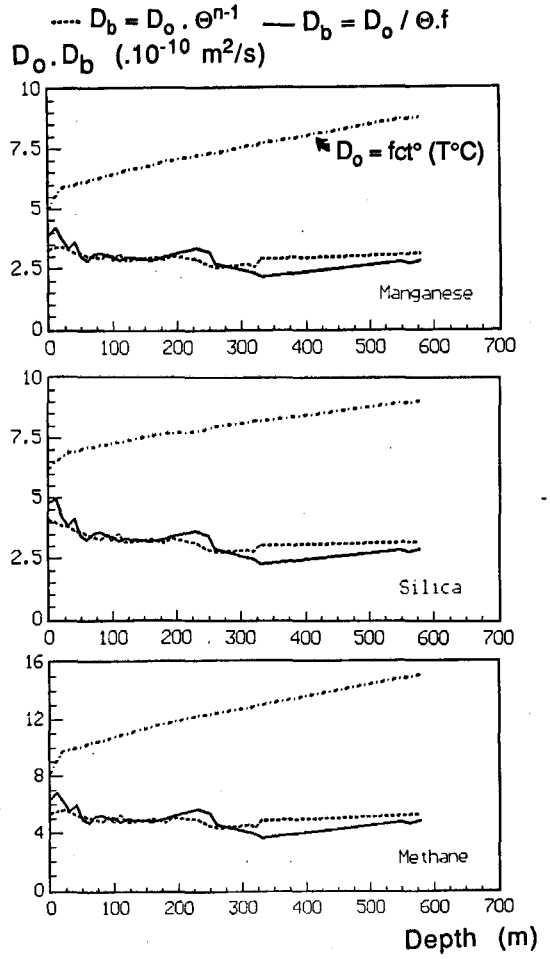

Figure 7

Methane, manganese and silica D_b values vs. *depth profiles; Site 671.*

Profils des coefficients de diffusion (D_b) du méthane, de manganèse et de la silice en fonction de la profondeur; Site 671.

Archie coefficient (n), the tortuosity (Φ), the porosity (θ), the formation factor (F) and the temperature (T). The variations of these parameters *versus* depth are shown for the site 671, as an example (Fig. 6). To obtain the best estimation of the molecular diffusion coefficients along the sedimentary sequence, D_b values were determined in using available data for the equation (8) and (10), respectively. Note in the Figure 7 that methane, manganese and silica Db values-depth profiles (site 671), which are calculated with the equation in using the Archie coefficients, are similar to those determinated with the equation using the formation factors. Hence, we postulate that the calculated D_b values are correct. Furthemore, several computational tests indicate that a deviation of about one unit of D_b values does not significantly change the obtained theoretical profiles.

Values for the advection fluid velocity have to be defined to test whether there is an upward fluid advection eventually acting above a structural pathway. However, the advection velocity values cannot be constrained by other quantitative parameters. For this reason, the effects of the diffusion processes were tested first by assuming that the vertical advection velocity equals zero. In this case, only diffusion processes would cause a dispersion of the chemical components from a fluid conduit toward the surrounding sediment.

RESULTS AND DISCUSSION

The results of the diffusion model are shown in the figures 8, 9, 10 at sites 671, 676 and 672 respectively. In these diagrams, the theoretical diffusion profiles obtained by computation match fairly well the analytical data profiles (Fig. 6, 7, 8). However, at some depths of sites 671 and 676, methane data cannot be explained by a simple diffusion model. This discrepancy can best be understood in terms of diagenetic processes involving methane consumption in the sedimentary sequence (Blanc *et al.* 1991). The similarity between theoretical and analytical concentration-depth profiles is, therefore, realized for average ages of the chemical anomalies characterizing each studied site. Estimation of the age for site 671 is 30,000 ± 10,000 years (Fig. 8). The positive chemical anomalies appear to have occurred since 7,000 ± 2,000 years at site 676 (Fig. 9), and 5,000 ± 1,000 years at site 672 (Fig. 10). In accordance with the Barbados accretionary prism development, the modelling suggests that ages should become younger from site 671, located 5 km west of the deformation front, towards site 672 located 6,2 km east of the deformation front. Considering a two-dimensional model of fluid circulation, a time of about 2,000 ± 1,000 years seems to be necessary for fluid flowing from the protodécollement zone beneath site 676 toward that beneath site 672. In order for fluid to travel 6,200 metres in 2,000 ± 1,000 years, it must flow 1.3 (± 0.7). 10^{-7} $m.s^{-1}$. A similar calculation between site 671 and site 676, which are five kilometres apart, suggests that the time necessary for the fluid flow is about 23,000 ± 8,000 years, and a fluid flow velocity ranging from 16 to 33 cm. yr^{-1}, or about 7.5 (± 3.0) . 10^{-9} $m.s^{-1}$. The discrepancy by a factor of about 20 between the calculated fluid flow velocities can be related to the difference in permeability along the décollement, within the toe part of the wedge, and in the protodécollement within the oceanic domain. Permeability is a factor of physical properties (depth of burial, grain size, porosity, bulk density) that affect the consolidation process and is dependent on the *in situ* stress field. Using physical parameters determined during Leg 110, Taylor and Leonard (1990) showed that the sediment permeabilities at site 671 calculated as hydraulic conductivities, are lower than that at site 672 by one to three orders of magnitude. Our estimate of the fluid flow velocity along the protodécollement (1.3 (± 0.7) . 10^{-7} $m.s^{-7}$) is also similar to that estimated by a simple thermal model, (*i.e.* 2. 10^{-7} $m.s^{-1}$) calculating how long it takes for a fluid, at the protodécollement depth, to cool from 22 to 17°C between site 676 and site 672 (Fisher and Hounslow, 1990). The estimated maximum sediment permeability within the protodécollement zone, which was based on the above fluid flow velocity, is about 10^{-12} m^2. In ODP Leg 110, near 15,4 °N, Le Pichon *et al.* (1990) and Wuthrich *et al.* (1990), considering numerical dewatering steady-state models within the first 35 km of the wedge, show that the excess of water within the subducted layer is essentially evacuated through the décollement with a velocity of about 10 $cm.yr^{-1}$ (*i.e.* 3. 10^{-9} $m.s^{-1}$). This velocity value is comparable to that which we have estimated between site 671 and site 676, and it requires intrinsic permeability values ranging between 10^{-14} and 10^{-15} m^2.

Figure 8

Left: theoretical concentration-depth profiles of methane, silica and manganese, in comparison with analytical data; right: structural and lithological data; site 671.

A gauche : profils théoriques des concentrations en méthane, silice and manganèse en fonction de la profondeur comparés aux données analytiques, à droite sont reportées les données issues des études lithologiques et structurales ; Site 671.

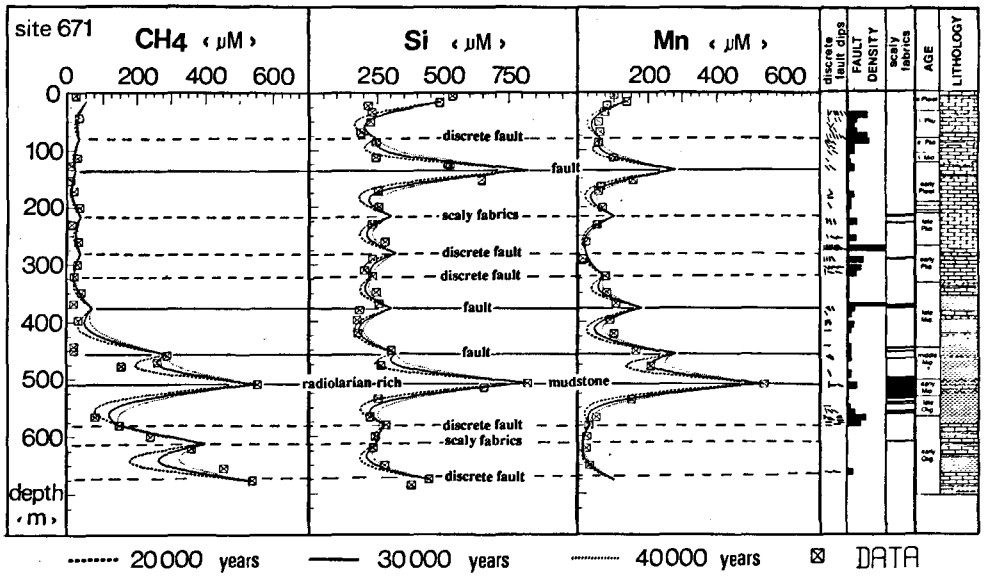

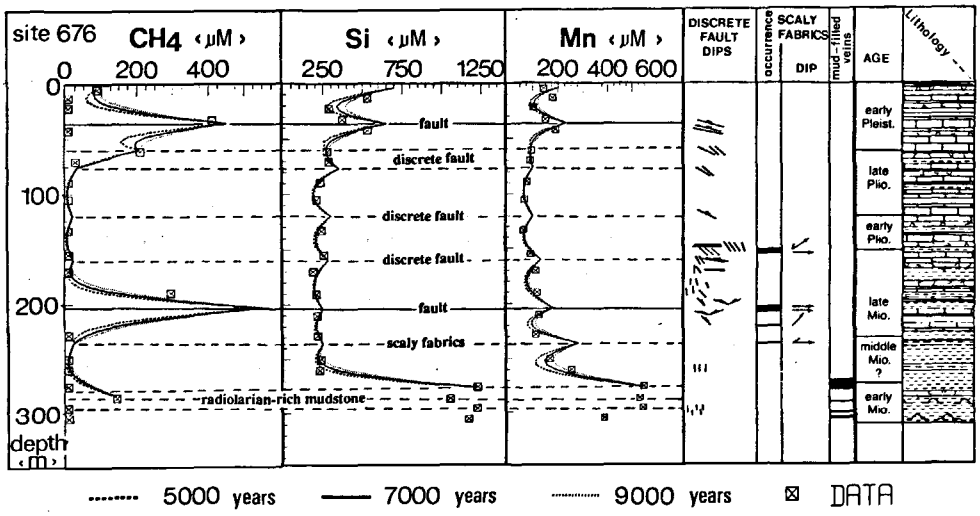

Figure 9

Left: theoretical concentration-depth profiles of methane, silica and manganese in comparison with analytical data; right: structural and lithological data; site 676.

A gauche : profils théoriques des concentrations en méthane, silice and manganèse en fonction de la profondeur comparés aux données analytiques, à droite sont reportées les données issues des études lithologiques et structurales ; Site 676.

Figure 10

Left: theoretical concentration-depth profiles of methane, silica and manganese in comparison with analytical data; rigth: structural and lithological data; site 672.

A gauche : profils théoriques des concentrations en méthane, silice and manganèse en fonction de la profondeur comparés aux données analytiques, à droite sont reportées les données issues des études lithologiques et structurales ; Site 672.

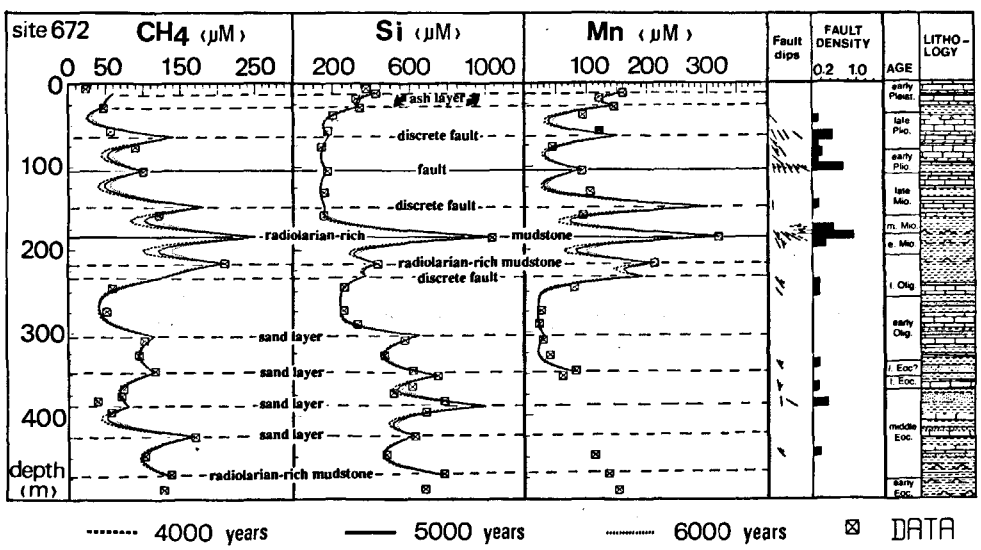

However, variation in lateral permeability distributions cannot directly explain why fluid flow velocity is higher between site 676 and site 672 than that between sites 671 and 676. Wuthrich *et al.* (1990) showed that the contrast between the equivalent décollement permeability (K_d) and the equivalent prism permeability (K_p) greatly affect the magnitude of pore fluid pressure, and hence, the pore-pressure ratio λ, in the complex. The pore-pressure ratio λ, represents the ratio of excess fluid pressure. Average λ in the décollement decreases arcward from the oceanic domain despite an increase in fluid pressure resulting from the arcward thickening in the prism (Wuthrich *et al.*, 1990).

The λ values within the propagating décollement in the oceanic domain seem to be, therefore, higher than those within the décollement in the toe part of the complex. This may help to explain why the propagating décollement can accomodate higher rates of fluid flow than the décollement itself.

An additional vertical advection can affect a profile by displacement and flattening the anomalies. The flux of water due to upward advection of fluid from the considered fluid conduits towards the surrounding sediments, can be assessed using our numerical model. We have checked the fit of the model to data by varying the upward advection velocity. Fit can only be obtained for upward velocity equal or less than 1.10^{-11} m.s^{-1} (*i.e.* ≈ 0.3 mm.yr^{-1}). Similar upward velocity values were determined by Wuthrich *et al.* (1990). The use of this range of low vertical velocity values does not significantly change the obtained theoretical profiles which remain comparable to the analytical chemical distributions relative to depth. Hence, the estimated times necessary to obtain a fit between theoretical and analytical profiles remain identical to those estimated in using an upward advection velocity equal to 0.

CONCLUSIONS

Our non-steady state diffusion-advection model describes well the concentration-depth profiles of methane, manganese and silica dissolved in the interstitial water samples collected during ODP Leg 110. Major and small-scale tectonic structures, and also, more permeable lithological layers seem to act as fluid conduits. The distribution of the chemical concentrations above and below these fluid conduits is apparently controlled by molecular diffusion processes. Upward fluid flow eventually occurring through the sediment prism appears to be very low in intensity, i.e. 1. 10^{-11} m.s^{-1} or less. Estimates of the time necessary to obtain fittings between theoretical and analytical profiles, defined average ages of the chemical anomalies characterizing each studied sites, as following: 30,000 ± 10,000 years at site 671, 7,000 ± 2,000 years at site 676, and 5,000 ± 1,000 years at site 672. This enables us to calculate fluid velocities along the décollement and protodécollement zones which are of the order of 7.10^{-9} and 1.10^{-7} m.s^{-1}, respectively. These fluid flow velocity values are comparable to those given by previous studies on the basis of thermal and mechanical behaviour of the accretionnary prism. The change in velocities can be related to pore-pressure ratios in the décollement, which increase seaward from site 671. Association of the most positive manganese anomalies with those of silica can be best understood in terms of dissolution of biogenic silica and manganese oxide with further precipitation of rhodochrosite.

Acknowledgements

We are grateful to anonymous reviewers for their constructive comments and suggestions for the improvement of the manuscript. A. Poulain (ENS des Mines, Fontainebleau) is thanked for discussions helpful in the establishment of the computering code. This research was supported by an internal grant from the *Centre de Géochimie de la Surface.*

REFERENCES

Archie G.E. (1942). The electrical resistivity log as an aid in determining some reservoirs characteristics. *Am. Inst. Mech. Engng Tr.*, **146**, 54-61.

Bear J. (1972). *Dynamics of fluid in porous media.* American Elsevier, New York, USA.

Behrmann J.H., K. Brown and Leg 110 Shipboard Scientific Party (1988). Evolution of structures and fabrics in the Barbados Accretionary Prism. *Journal of Structural Geology, vol. 10.* Pergamon Press, Oxford, UK, 577-591.

Blanc G., J.M. Gieskes and ODP Leg 110 Scientific Party (1988). Advection de fluides interstitiels dans les séries sédimentaires du complexe d'accrétion de la Barbade (Leg 110 ODP). *Bull. Soc. géol. Fr.*, **8**, 453-460.

Blanc G. J. Boulègue and J.M. Gieskes (1991). Chemical evidence for advection of interstitial fluid in the sedimentary series of the Barbados accretionary complex (Leg 110). *Oceanologica Acta*, **14**, 1, 33-49.

Brown K.M. and J.H. Behrmann (1990). Genesis and evolution of small-scale structures in the toe of the Barbados ridge accretionary wedge. in: *Proceedings ODP, Scientific Results, 110*, J.C. Moore, A. Mascle *et al.*, editors. College Station, Texas, USA, 229-244.

Brown K.M., A. Mascle and J.H. Behrmann (1990). Mechanisms of accretion and subsequent thickening in the Barbados ridge accretionary complex: Balanced cross sections across the wedge toe. in: *Proceedings ODP, Scientific Results, 110*, J.C. Moore, A. Mascle *et al.*, editors. College Station, Texas, USA, 209-227.

Fisher A.T. and M.W. Hounslow (1990 *a*). Heat flow through the toe of the Barbados accretionary complex. in: *Proceedings ODP, Scientific Results, 110*, J.C. Moore, A. Mascle *et al.*, editors. College Station, Texas, USA, 345-360.

Fisher A.T. and M.W. Hounslow (1990 *b*). Transient fluid flow through the toe of the Barbados accretionary complex: constraints from Ocean Drilling Program Leg 110. Heat flow studies and simple models. *J. geophys. Res.*, **95**, B6, 8845-8858.

Fritz B. (1981). Étude thermodynamique et simulations des réactions hydrothermales et diagénétiques. *Mém. Sci. géol., Strasbourg*, **65**, 197 pp.

Gieskes J.M., G. Blanc and Leg 110 Shipboard Scientific Party (1989). Hydrogeochemistry in the Barbados Accretionary Complex: Leg 110 ODP. *Paleogeogr. Paleoclimatol. Paleoecol.*, **71**, 83-96.

Gieskes J.M., G. Blanc, P. Vrolijk, H. Elderfield and R. Barnes (1990 *a*). Interstitial water chemistry major constituents. in: *Proceeding ODP, Scientific Results, 110*, J.C. Moore, A. Mascle *et al.*, editors. College Station, Texas, USA, 155-178.

Gieskes J.M., P. Vrolijk and G. Blanc (1990 *b*). Hydrogeochemistry of the Northern Barbados Accretionary Complex Transect: ODP Leg 110. *J. geophys. Res.*, **95**, B6, 8809-8818.

Klinkenberg L.J. (1951). Analogy between diffusion and electrical conductivity in porous rocks. *Geol. Soc. Am. Bull.*, **62**, 559-563.

Le Pichon X., P. Henry and S. Lallemant (1990). Water flow in the Barbados accretionary complex. *J. geophys. Res.*, **95**, B6, 8945-8967.

Lerman A. (1979). Fluxes and transport: molecular diffusion. in: *Geochemical processes water and sediment environments.* John Wiley and Sons, Ed. Wiley Interscience Pub., 73-110.

Li Y.H. and S. Gregory (1974). Diffusion of ions in sea water and in deep-sea sediments. *Geochim. cosmochim. Acta*, **38**, 703-714.

Manheim F.T. (1970). The diffusion of ions in unconsolidated sediments. *Earth planet. Sci. Letts*, **9**, 307-309.

Manhein F.T. and L.S. Waterman (1974). Diffusimetry (diffusion constant estimation) on sediment cores by resistivity probe. in: *Reports of the DSDP, vol. 22.* US Journal Printing Office, Washington, D.C., USA, 663-670.

de Marsily G. (1981). *Hydrologie quantitative.* Masson Ed., Paris, 163 pp.

Mascle A., J.C. Moore and Leg 110 Shipboard Scientific Party (1988). Proceedings ODP, Initial reports. Part A, 110, College Station, TX (Ocean Drilling Programme), 603.

Moore J.C., A. Mascle and Leg 110 Shipboard Scientific Party (1988). Tectonics and Hydrogeology of the Northern Barbados Ridge: Result from Leg 110 ODP. *Geol. Soc. Am. Bull.*, **100**,10, 1578-1593.

ODP Leg 110 Scientific Party (1987). Expulsion of deep-sourced fluids along subduction zone décollement northern Barbados ridge. *Nature*, **326**, 6115, 785-788.

Ogata A. and R.B. Banks (1961). A solution of the differential equation of longitudinal dispersion in porous media. *U.S. Geol. Surv. Open-file Rept*, **411 A**, 1-7.

Schoonmaker-Tribble J. (1990). Clay diagenesis in the Barbados accretionary complex: potential impact of hydrology and subduction dynamics. in: *Proceedings ODP, Scientific Results, 110*, J.C. Moore, A. Mascle *et al.*, editors. College Station, Texas, USA, 97-110.

Taylor E. and J. Leonard (1990). Sediment consolidation and permeability at the Barbados Forearc. in: *Proceedings ODP, Scientific Results, 110*, J.C. Moore, A. Mascle *et al.*, editors. College Station, Texas, USA, 289-308.

Vrolijk P. and S.M.F. Sheppard (1991). Syntectonic carbonate veins from the Barbados accretionary prism (ODP Leg 110): record of paleohydrology. *Sedimentology*, **38**, 671-690.

Vrolijk P., S.R. Chambers, J.M. Gieskes and J.R. O'Niel (1990). Stable isotope ratios of interstitial fluids from the Northern Barbados Accretionary Prism, ODP Leg 110, in: *Proceedings ODP, Scientific Results, 110*, J.C. Moore, A. Mascle *et al.*, editors. College Station, Texas, USA, 189-205.

Wuthrich D.R., E.J. Screaton and S.J. Dreiss (1990). Fluid flow within the Barbados ridge complex, permeability estimates and numerical simulations of flow velocities and pore pressures. in: *Proceedings ODP, Scientific Results, 110*, J.C. Moore, A. Mascle *et al.*, editors. College Station, Texas, USA, 331-344.